On motions that allow for identification of hinge joint axes from kinematic constraints and 6D IMU data

Nowka, Danny; Kok, Manon; Seel, Thomas

Important note
To cite this publication, please use the final published version (if applicable).
Please check the document version above.

On Motions That Allow for Identification of Hinge Joint Axes from Kinematic Constraints and 6D IMU Data

Danny Nowka[1], Manon Kok[2], Thomas Seel[1]

Abstract— In inertial motion tracking of kinematic chains, inertial measurement units (IMUs) are attached to each segment in order to track their motion in three-dimensional space. Determining the relations between the functional axes of a joint and the local coordinate system of the attached sensor is a crucial requirement. For the case of hinge joints, methods have been proposed that exploit kinematic constraints to automatically identify the local hinge joint axis coordinates from the raw data of almost arbitrary motions. However, to current date, it remains unclear which joint motions are sufficiently rich for the joint axis to become identifiable. We consider a commonly used gyroscope-based kinematic constraint and present a novel accelerometer-based kinematic constraint. We study conditions of identifiability by analyzing the nonlinear constraint equations and present practical conditions for the minimum excitation that is required. Among other results, we prove that planar motions and subsequent motions of both ends of the joint are sufficient as long as the joint axis does not remain perfectly horizontal. Theoretical results are validated in experimental studies of a human upper limb wearing an exoskeleton. Despite the typical IMU-related measurement inaccuracies and although the human elbow joint is only an approximate hinge joint, the cost function defined by the kinematic constraints exhibits a distinct global minimum at the true joint axis coordinates if the motion fulfills the proposed requirements.

I. INTRODUCTION

In recent years, the importance of miniature inertial measurement units (IMUs) for motion tracking is increasing rapidly across different application fields due to improved accuracy, cost and flexibility. Common use cases include human motion analysis [1], [2], vehicle motion state estimation [3], [4], robotics [5], [6] and real-time motion tracking for feedback control of exoskeletons and neuroprostheses [7], [8]. In many of these applications, IMUs are used to track the motion of a kinematic chain, i.e. a number of rigid segments that are pairwise interconnected by joints with one, two or three rotational degrees of freedom.

When inertial sensors are attached to the segments, the local measurement coordinate systems of the sensors are, in general, not well aligned with the functional joint axes. Figure 1 illustrates this fact for the example of a hinge joint, i.e. a joint with one rotational degree of freedom. In order to determine useful kinematic quantities from the sensor readings, one must identify the relation between the functional axes of the joint and the sensor coordinate systems. In human motion tracking, this process is sometimes called anatomical calibration. Both in mechatronic systems and in

[1]Danny Nowka and Thomas Seel are with Control Systems Group at Technische Universität Berlin, seel@control.tu-berlin.de.
[2]Manon Kok is with the Delft Center for Systems and Control, Delft University of Technology, the Netherlands, m.kok-1@tudelft.nl.
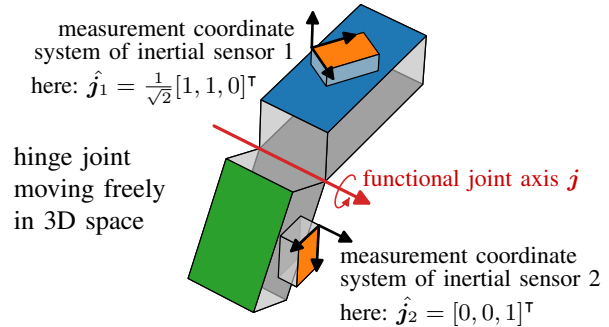
Fig. 1: Model of two rigid segments connected by a hinge joint. An IMU is attached to each segment with an unknown orientation. Under certain conditions, the joint axis coordinates $\hat{\boldsymbol{j}}_1, \hat{\boldsymbol{j}}_2$ can be identified from measured raw data.

human motion tracking, a standard solution is to perform a precise motion of the joint around isolated degrees of freedom prior to the actual motion of interest. The local joint axis coordinates are then identified from the measurements taken during this precise calibration motion, see e.g. [9]–[11]. Obviously, the accuracy of such a calibration crucially depends on the precision of the performed motion.

In many applications, including human motion tracking, it seems desirable to overcome this limitation and to enable sensor-to-segment calibration from more arbitrary motions, see e.g. [12], [13]. It is often even desirable to supersede calibration motions entirely by identifying the joint axis coordinates directly from the data of the actual motion of interest, which is sometimes called *plug-and-play* motion tracking. This goal has been pursued in a number of publications proposing algorithms that exploit kinematic constraints to identify the joint axis coordinates from data of not precisely defined motions. For the case of hinge joints, methods have been proposed for joint axis and position identification [14], for joint angle estimation [15], and for sensor-to-joint position estimation [16]. Similar approaches have recently been studied for two-dimensional joints [17], [18]. While several experimental proofs of concept have been provided for certain types of motion of certain joints, previous work lacks a thorough analysis of the conditions that a motion must fulfill to render the joint axis coordinates identifiable. For example, a motion with a constant joint angle – i.e. without relative motion between both ends of the joint – is not sufficient for joint axis identification, since the joint behaves like a single rigid body. In contrast, moving the joint along all degrees of freedom is intuitively expected to yield sufficient excitation.

The current contribution considers one-dimensional joints and provides a rigorous analysis of the uniqueness of solutions under different motions. Beside the commonly used gyroscope-based constraint, we propose an accelerometer-based constraint. This constraint facilitates exploitation of kinematic constraints for motions with small velocity changes, i.e. motions for which the accelerometer measurement is dominated by the gravity, and complements the gyroscope-based constraints, especially for motions with small angular velocities. We analyze the set of nonlinear constraint equations for multiple samples taken during a motion and study conditions that the measured acceleration and angular rate must fulfill to make the joint axis coordinates identifiable.

The remainder of this contribution is organized as follows. In Section II the mechanical model is explained, the optimization-based approach for joint axis identification by exploitation of kinematic constraints is reviewed briefly, and the novel constraint is introduced. In Section III we formulate our problem description. In Section IV we analyze the set of nonlinear constraint equations for multiple samples taken during a motion and study conditions that the measured acceleration and angular rate must fulfill to assure that this set of equations has a unique solution. Finally, in Section V, we validate the theoretical results experimentally using a mechanical and a biological joint.

II. KINEMATIC MODEL AND CONSTRAINTS

A. Kinematic Model of a Hinge Joint System

The hinge joint is modeled as shown in Figure 1. Two rigid segments represent both ends of the joint and are mechanically linked such that there remains one rotational degree of freedom in between. The system can be in any orientation w.r.t. an inertial frame $\mathcal{E}$, i.e. it has four rotational degrees of freedom in total. The joint axis is represented by the unit-length joint axis vector, whose coordinates in the inertial frame are denoted $\boldsymbol{j}$. Obviously, $-\boldsymbol{j}$ represents the same joint axis. An IMU is rigidly attached to each segment with an arbitrary orientation. The corresponding intrinsic measurement frames of the sensors are denoted by $\mathcal{S}_1$ and $\mathcal{S}_2$.

The coordinates of the joint axis in frames $\mathcal{S}_1$ and $\mathcal{S}_2$ are denoted by $\boldsymbol{j}_1$ and $\boldsymbol{j}_2$, respectively. Since the inertial sensors remain rigidly attached to the segments during any motion, $\boldsymbol{j}_i, i \in \{1, 2\}$, are constant parameters that describe the time-invariant relation between the inertial sensor and the functional joint axis. This relation must be known in order to calculate meaningful kinematic quantities, e.g. joint angles.

Both sensors provide measurement of the acceleration $\boldsymbol{a}_i$ and angular velocity $\boldsymbol{\omega}_i$, where the subscript $i \in \{1, 2\}$ indicates the corresponding sensor $\mathcal{S}_i$. In the following we assume all measurement errors and noise to be negligible. As explained above, we aim to determine $\boldsymbol{j}_1$ and $\boldsymbol{j}_2$ from these measurements of the inertial sensors. This can be achieved by exploitation of kinematic constraints.

B. Gyroscope-based Kinematic Constraint

We first review the gyroscope-based constraint proposed in [14]. Given any angular velocity of the first sensor $\boldsymbol{\omega}_1$, the second sensor's angular velocity must be

$$\boldsymbol{\omega}_2(t) = \boldsymbol{R}(t)\boldsymbol{\omega}_1(t) + \dot{\alpha}(t)\boldsymbol{j}_2, \tag{1}$$

where $\alpha(t)$ is the unknown joint angle and $\boldsymbol{R}(t)$ is an unknown time-variant rotation matrix that describes the relative orientation of $\mathcal{S}_1$ and $\mathcal{S}_2$. Note that $\boldsymbol{\omega}_2$ can be decomposed into a rotation around the joint axis and a portion perpendicular to the joint axis, i.e. trivially

$$\boldsymbol{\omega}_2(t) = (\boldsymbol{j}_2^{\mathsf{T}}\boldsymbol{\omega}_2(t)\boldsymbol{j}_2) + (\boldsymbol{\omega}_2(t) - \boldsymbol{j}_2^{\mathsf{T}}\boldsymbol{\omega}_2(t)\boldsymbol{j}_2). \tag{2}$$

Using (1), we rewrite the first term as follows

$$\begin{aligned}
\boldsymbol{j}_2^{\mathsf{T}}\boldsymbol{\omega}_2(t)\boldsymbol{j}_2 &= \boldsymbol{j}_2^{\mathsf{T}}(\boldsymbol{R}(t)\boldsymbol{\omega}_1(t))\boldsymbol{j}_2 + \boldsymbol{j}_2^{\mathsf{T}}(\dot{\alpha}(t)\boldsymbol{j}_2)\boldsymbol{j}_2 \\
&= \boldsymbol{j}_2^{\mathsf{T}}(\boldsymbol{R}(t)\boldsymbol{\omega}_1(t))\boldsymbol{j}_2 + \dot{\alpha}(t)\boldsymbol{j}_2, \tag{3}
\end{aligned}$$

and find the second term on the right-hand side of (2) to be

$$\boldsymbol{\omega}_2(t) - \boldsymbol{j}_2^{\mathsf{T}}\boldsymbol{\omega}_2(t)\boldsymbol{j}_2 = \boldsymbol{R}(t)\boldsymbol{\omega}_1(t) - \boldsymbol{j}_2^{\mathsf{T}}(\boldsymbol{R}(t)\boldsymbol{\omega}_1(t))\boldsymbol{j}_2.$$

Since by definition $\boldsymbol{j}_2 = \boldsymbol{R}(t)\boldsymbol{j}_1$, we obtain the relation

$$\boldsymbol{\omega}_2(t) - \boldsymbol{j}_2^{\mathsf{T}}\boldsymbol{\omega}_2(t)\boldsymbol{j}_2 = \boldsymbol{R}(t)\big(\boldsymbol{\omega}_1(t) - \boldsymbol{j}_1^{\mathsf{T}}\boldsymbol{\omega}_1(t)\boldsymbol{j}_1\big).$$

To eliminate the rotation matrix $\boldsymbol{R}(t)$, we take the Euclidean norm on both sides, which is invariant under rotation:

$$\left\|\boldsymbol{\omega}_2(t) - \boldsymbol{j}_2^{\mathsf{T}}\boldsymbol{\omega}_2(t)\boldsymbol{j}_2\right\|_2 = \left\|\boldsymbol{\omega}_1 - \boldsymbol{j}_2^{\mathsf{T}}\boldsymbol{\omega}_1(t)\boldsymbol{j}_2\right\|_2. \tag{4}$$

Since $\boldsymbol{j}_1, \boldsymbol{j}_2$ have unit length, this is equivalent to

$$\left\|\boldsymbol{\omega}_1(t) \times \boldsymbol{j}_1\right\|_2 = \left\|\boldsymbol{\omega}_2(t) \times \boldsymbol{j}_2\right\|_2. \tag{5}$$

Note that this reasoning holds for each moment in time. The constraint (5) must therefore be fulfilled by all gyroscope readings of any motion of a hinge joint system. It is a compact equation that couples the parameters of interest directly with the raw data without requiring strapdown integration or any type of sensor fusion. However, (5) is nonlinear in both $\boldsymbol{j}_i$ and $\boldsymbol{\omega}_i, i = 1, 2$. Moreover, the terms are invariant with respect to the signs of $\boldsymbol{j}_1$ and $\boldsymbol{j}_2$. Therefore, the constraint is always fulfilled by the two correct axis coordinate pairs $(\boldsymbol{j}_1, \boldsymbol{j}_2)$ and $(-\boldsymbol{j}_1, -\boldsymbol{j}_2)$ as well as by two coordinate pairs $(-\boldsymbol{j}_1, \boldsymbol{j}_2)$ and $(\boldsymbol{j}_1, -\boldsymbol{j}_2)$ that suffer from non-matching signs, cf. [12]. While practical solutions have been proposed to match the signs, it seems desirable to find a constraint that allows discrimination between the two correct and the two false sign combinations.

C. Accelerometer-based Kinematic Constraint

We now present a novel kinematic constraint that is based on accelerometer readings. Accelerometers measure the specific force, which is the acceleration due to change of velocity plus an acceleration due to gravity acting on the proof mass of the accelerometer. When velocity changes are much smaller than $9.8 \frac{\text{m}}{\text{s}^2}$, the acceleration measurements can accurately be approximated to solely represent the gravity vector, which implies that

$$\boldsymbol{a}_2(t) \approx \boldsymbol{R}(t)\boldsymbol{a}_1(t). \tag{6}$$

4326

We exploit the fact that the inner product is invariant under rotation. Taking the inner product with $\boldsymbol{j}_2$ on both sides yields

$$\boldsymbol{j}_2^\mathsf{T} \boldsymbol{a}_2(t) = \boldsymbol{j}_2^\mathsf{T} \boldsymbol{R}(t)\boldsymbol{a}_1(t) = \boldsymbol{j}_1^\mathsf{T} \boldsymbol{a}_1(t), \tag{7}$$

i.e. the projections of the measured accelerations onto the joint axis must have same length for all t. Mathematically similar constraints have been used by [16] and by [19]. The acceleration-based constraint has three main advantages:

- It does not require strapdown integration or orientations,
- it is linear in both $\boldsymbol{j}_i$ and $\boldsymbol{a}_i$, and
- unlike (5), it is sign-sensitive in the sense that

$$\boldsymbol{j}_2^\mathsf{T} \boldsymbol{a}_2(t) = \boldsymbol{j}_1^\mathsf{T} \boldsymbol{a}_1(t) \Rightarrow (-\boldsymbol{j}_2)^\mathsf{T} \boldsymbol{a}_2(t) = (-\boldsymbol{j}_1)^\mathsf{T} \boldsymbol{a}_1(t)$$
$$\not\Rightarrow \boldsymbol{j}_2^\mathsf{T} \boldsymbol{a}_2(t) = (-\boldsymbol{j}_1)^\mathsf{T} \boldsymbol{a}_1(t)$$
$$\not\Rightarrow (-\boldsymbol{j}_2)^\mathsf{T} \boldsymbol{a}_2(t) = \boldsymbol{j}_1^\mathsf{T} \boldsymbol{a}_1(t).$$

The main disadvantage of the accelerometer-based constraint is that it only holds if the change of velocity, i.e. also the rotation, is negligible in both sensors. In Section V we will evaluate the usefulness of the constraint for typical human upper limb motions.

III. PROBLEM FORMULATION

We formulate the problem of axis identification as a set of nonlinear equations. Consider a perfect hinge joint system with measurements $\boldsymbol{a}_i(t_k), \boldsymbol{\omega}_i(t_k), k = 1, 2, ..., N$ taken by both sensors $i = 1, 2$, at N sample instants. We then find the following set of constraint equations:

$$\boldsymbol{j}_1^\mathsf{T}\boldsymbol{j}_1 = \boldsymbol{j}_2^\mathsf{T}\boldsymbol{j}_2 = 1, \tag{8}$$
$$h_1(t_k) = h_2(t_k) = 0 \ \forall k \in \{1, 2, ..., N\}, \tag{9}$$
$$h_1(t_k) := \|\boldsymbol{\omega}_1(t_k) \times \boldsymbol{j}_1\|_2 - \|\boldsymbol{\omega}_2(t_k) \times \boldsymbol{j}_2\|_2, \tag{10}$$
$$h_2(t_k) := \boldsymbol{j}_1^\mathsf{T}\boldsymbol{a}_1(t_k) - \boldsymbol{j}_2^\mathsf{T}\boldsymbol{a}_2(t_k). \tag{11}$$

Obviously, there are always at least two pairs of joint axis coordinates that fulfill all of these constraint equations: the true joint axis coordinates $(\hat{\boldsymbol{j}}_1, \hat{\boldsymbol{j}}_2)$ and the equivalent pair $(-\hat{\boldsymbol{j}}_1, -\hat{\boldsymbol{j}}_2)$. However, if excitation is weak there might be other axis coordinate pairs that also fulfill (8) and (9). The core question of this contribution is which minimum requirements the motion, and thus the measured accelerations and angular rates, must fulfill to assure that (8), (9) hold only for the true joint axis coordinate pairs, i.e. to assure that the following properties hold:

Definition 1 (Uniqueness of the Axis): The axis identification problem has a unique solution if $(\hat{\boldsymbol{j}}_1, \hat{\boldsymbol{j}}_2)$ and $(-\hat{\boldsymbol{j}}_1, -\hat{\boldsymbol{j}}_2)$ are the only coordinates that fulfill (8) and (9).

Definition 2 (Uniqueness of the Axis up to Sign Pairing): The axis identification problem has a unique solution up to sign pairing if $(\hat{\boldsymbol{j}}_1, \hat{\boldsymbol{j}}_2)$, $(-\hat{\boldsymbol{j}}_1, \hat{\boldsymbol{j}}_2)$, $(\hat{\boldsymbol{j}}_1, -\hat{\boldsymbol{j}}_2)$, and $(-\hat{\boldsymbol{j}}_1, -\hat{\boldsymbol{j}}_2)$ are the only coordinates that fulfill (8) and (9).

IV. CONDITIONS ON ARBITRARY MOTIONS FOR JOINT AXIS IDENTIFICATION

We first discuss two cases that clearly have insufficient excitation to uniquely identify the joint axis.

- Both segments are *stationary*.

- The segments *move jointly* but do not move with respect to each other.

Subsequently, we will discuss the case where the joint only moves slowly and the angular velocities are negligible. We analyze when the joint axis is identifiable from the accelerometer constraint. Finally, we discuss the case where both the gyroscope- and the accelerometer-based constraints can be used. Again, we will discuss two special cases:

- *Sequential motion*: Motion that contains, for each segment, a (potentially very short) period of time during which only that segment moves.
- *Simultaneous planar motion*: Motion during which, at least for some time periods, both segments of the joint rotate simultaneously but in the same fixed plane, i.e. in the joint plane that is perpendicular to the joint axis.

A. Insufficient Excitation

1) Stationary: Let us first consider the trivial case of a stationary hinge joint system that does not move at all. In this case, the gyroscope-based constraint (5) is trivially fulfilled for any $\boldsymbol{j}_1$ and $\boldsymbol{j}_2$. Furthermore, since the measured accelerations $\boldsymbol{a}_1, \boldsymbol{a}_2$ are time-invariant, the accelerometer-based constraint (7) yields the same linear equation for each sample instant. The set of solutions is therefore the intersection of the manifold defined by the constraints on the norms of $\boldsymbol{j}_1$ and $\boldsymbol{j}_2$, (8), and the affine hyperplane defined by the aforementioned single linear equation. These are infinitely many points. For instance, any unit vector $\boldsymbol{j}_1$ orthogonal to $\boldsymbol{a}_1$ in combination with any unit vector $\boldsymbol{j}_2$ orthogonal to $\boldsymbol{a}_2$ fulfill these constraints.

2) Joint Movement: A much more general case is a hinge joint system moving freely in three-dimensional space but with fixed joint angle, i.e. without relative motion between the segments. The relative orientation of both sensor frames can then be expressed by a time-invariant rotation matrix $\boldsymbol{R}$. Consider any arbitrary vector $\boldsymbol{j}_1$ and let $\boldsymbol{j}_2 = \boldsymbol{R}\boldsymbol{j}_1$. Then, with omission of time indices, we have

$$\boldsymbol{j}_2^\mathsf{T} \boldsymbol{a}_2 = (\boldsymbol{R}\boldsymbol{j}_1)^\mathsf{T}(\boldsymbol{R}\boldsymbol{a}_1) = \boldsymbol{j}_1\boldsymbol{R}^\mathsf{T}\boldsymbol{R}\boldsymbol{a}_1 = \boldsymbol{j}_1^\mathsf{T}\boldsymbol{a}_1,$$
$$\boldsymbol{\omega}_2 \times \boldsymbol{j}_2 = (\boldsymbol{R}\boldsymbol{\omega}_1) \times (\boldsymbol{R}\boldsymbol{j}_1) = \boldsymbol{R}(\boldsymbol{\omega}_1 \times \boldsymbol{j}_1),$$
$$\|\boldsymbol{\omega}_2 \times \boldsymbol{j}_2\|_2 = \|\boldsymbol{R}(\boldsymbol{\omega}_1 \times \boldsymbol{j}_1)\|_2 = \|\boldsymbol{\omega}_1 \times \boldsymbol{j}_1\|_2.$$

In other words, the kinematic constraints (9) are automatically fulfilled.

Result 1 (Insufficient Excitation): If there is no relative motion between both segments, there are infinitely many solutions to the constraints (8) and (9), which implies that the joint axis cannot be identified.

B. Motions with Negligible Angular Rates

Consider motions with slow rotations and at least short periods of (almost) constant velocity. For this case, rotation might be so slow that the measured angular rates are in the same order of magnitude as the measurement errors of the gyroscope. Hence, the value of the gyroscope-based constraint will be limited. Whenever velocity changes are small, the measured acceleration is clearly dominated by

gravity, and the accelerometer-based constraint is fulfilled. We therefore investigate uniqueness of the solution of

$$h_2(t_k) = 0 \; \forall \, k \in \{1, 2, ..., N\}, \quad \boldsymbol{j}_1^{\mathsf{T}} \boldsymbol{j}_1 = \boldsymbol{j}_2^{\mathsf{T}} \boldsymbol{j}_2 = 1. \quad (12)$$

Considering $h_2(t_k)$ for a set of N measurement samples yields the linear system

$$\begin{bmatrix} h_2(t_1) \\ \vdots \\ h_2(t_N) \end{bmatrix} = \underbrace{\begin{bmatrix} \boldsymbol{a}_1^{\mathsf{T}}(t_1) & -\boldsymbol{a}_2^{\mathsf{T}}(t_1) \\ \vdots & \vdots \\ \boldsymbol{a}_1^{\mathsf{T}}(t_N) & -\boldsymbol{a}_2^{\mathsf{T}}(t_N) \end{bmatrix}}_{\boldsymbol{A}} \begin{bmatrix} \boldsymbol{j}_1 \\ \boldsymbol{j}_2 \end{bmatrix} = \boldsymbol{0} \; . \quad (13)$$

The solution space of the linear system (13) is the kernel $\mathcal{K} := \ker(\boldsymbol{A})$. For perfect accelerometer measurements of a hinge joint system, the kernel cannot be empty, since the true axis coordinates $[\hat{\boldsymbol{j}}_1, \hat{\boldsymbol{j}}_2]^{\mathsf{T}}$ and their negative counterparts $[-\hat{\boldsymbol{j}}_1, -\hat{\boldsymbol{j}}_2]^{\mathsf{T}}$ must represent non-trivial solutions for (13). If the dimension of the kernel is equal to one, the solutions satisfying (13) will be given by a straight line passing through the origin of $\mathbb{R}^6$. Note that any such line can only contain two points that fulfill the norm constraints (8), since

$$\boldsymbol{j}_1^{\mathsf{T}} \boldsymbol{j}_1 = 1 \; \Rightarrow \; (\gamma \boldsymbol{j}_i)^{\mathsf{T}} (\gamma \boldsymbol{j}_i) \neq 1 \; \forall \, \gamma \in \mathbb{R} \setminus \{1, -1\}.$$

We therefore, conclude that

$$\dim(\mathcal{K}) = 1 \quad \Leftrightarrow \quad \mathrm{rank}(\boldsymbol{A}) = 5 \quad (14)$$

is a sufficient condition for uniqueness of the identified axis according to Definition 1.

Result 2 (Rank Condition): The joint axis coordinates can be uniquely determined from any motion that leads to five linearly independent rows $[\boldsymbol{a}_1^{\mathsf{T}}(t_k), -\boldsymbol{a}_2^{\mathsf{T}}(t_k)]$, where each t_k is a time instant with negligible change of velocities.

C. Motions with Non-Negligible Angular Rates

In this section we consider motions that contain at least some periods of rotation that result in angular rates that are large enough to neglect any measurement errors. Since this class of motions is very large, we will focus on two elementary motions that are often contained in more complex motions: a sequential motion of both segments and a simultaneous planar rotation of both segments. Note that it is not necessary to detect these elementary motions in the more complex motion. Instead, as suggested in [14], [16], one can simply use a large number of sampled data sets, minimize some vector norm of (9) for all time instants, and include (8) as equality constraints of the optimization. Samples that contain no additional information will then have only marginal influence on the result via measurement errors.

1) Sequential motion: Consider the case in which one segment remains fixed while the other segment rotates around the one remaining degree of freedom. Without loss of generality, assume that the rotating segment is the first segment. The gyroscope-based constraint then becomes

$$\|\boldsymbol{\omega}_1(t_k) \times \boldsymbol{j}_1\|_2 = 0 \; \forall \, k \in \{1, 2, ..., N\}, \quad (15)$$

where all angular rates $\boldsymbol{\omega}_1(t_k)$ are collinear. Note that the cross product of two vectors becomes zero only if the vectors

are collinear. Therefore, (15) can only have two unit-length solutions. This implies that the considered unilateral motion is sufficient for identification of $\boldsymbol{j}_1$ up to its sign.

Now consider a motion that contains, for each segment, a (potentially very short) time period during which only that segments moves. More precisely, $\exists t_1, t_2$ such that $\boldsymbol{\omega}_1(t_1) \neq \boldsymbol{0} = \boldsymbol{\omega}_2(t_1)$ and $\boldsymbol{\omega}_1(t_2) = \boldsymbol{0} \neq \boldsymbol{\omega}_2(t_2)$. Note that the cross product can be written as $\boldsymbol{\omega}_i(t_i) \times \boldsymbol{j}_i =: \boldsymbol{G}_i \boldsymbol{j}_i$. Hence,

$$\|\boldsymbol{\omega}_i(t_i) \times \boldsymbol{j}_i\|_2 = 0, \, i = 1, 2 \; \Leftrightarrow \; \boldsymbol{G}_i \boldsymbol{j}_i = \boldsymbol{0}, \, i = 1, 2. \quad (16)$$

Note that the equations for $\boldsymbol{j}_1$ and $\boldsymbol{j}_2$ are decoupled and that $\mathrm{rank}(\boldsymbol{G}_i) = 2$. Hence, combining (16) with the norm constraints (8) yields exactly four solutions: all four combinations of signs of $(\pm \hat{\boldsymbol{j}}_1, \pm \hat{\boldsymbol{j}}_2)$, which means only uniqueness up to sign pairing is achieved (cf. Definition 2).

Including the accelerometer-based constraints for the same time instants yields

$$\begin{bmatrix} \boldsymbol{G}_1 & \boldsymbol{0} \\ \boldsymbol{0} & \boldsymbol{G}_2 \\ \boldsymbol{a}_1^{\mathsf{T}}(t_1) & -\boldsymbol{a}_2^{\mathsf{T}}(t_1) \\ \boldsymbol{a}_1^{\mathsf{T}}(t_2) & -\boldsymbol{a}_2^{\mathsf{T}}(t_2) \end{bmatrix} \begin{bmatrix} \boldsymbol{j}_1 \\ \boldsymbol{j}_2 \end{bmatrix} = \boldsymbol{0}. \quad (17)$$

This matrix must have rank five unless the last two rows are perpendicular to all sign combinations of $[\pm \hat{\boldsymbol{j}}_1, \pm \hat{\boldsymbol{j}}_2]^{\mathsf{T}}$, which can only be true if

$$\hat{\boldsymbol{j}}_1^{\mathsf{T}} \boldsymbol{a}_1(t_i) = \hat{\boldsymbol{j}}_2^{\mathsf{T}} \boldsymbol{a}_2(t_i) = 0 \; \forall \, i \in \{1, 2\}. \quad (18)$$

This represents the singular case in which the joint axis is perfectly horizontal at t_1 and at t_2.

Result 3 (Sequential Motions): The joint axis coordinates can be determined *up to sign pairing* if the motion contains isolated rotations of both segments. If, moreover, the motion contains at least one time instant at which the joint axis is not perfectly horizontal, then the joint axis coordinates can be determined *uniquely* in the sense of Definition 1.

2) Simultaneous Planar Motion: Consider a motion during which, at least for some periods of time, both segments of the joint rotate simultaneously but in the same plane, i.e. in the joint plane that is perpendicular to the joint axis. The motion of a human leg during walking is an example of this type of motion if the thigh and shank move in the sagittal plane during some periods of the gait cycle.

If such a planar motion is performed during a potentially very short time interval $[t_1, t_2]$, then there must exist two scalars $c_1, c_2 \in \mathbb{R} \setminus \{0\}$ such that

$$\boldsymbol{\omega}_1(t_2) = c_1 \boldsymbol{\omega}_1(t_1), \quad \boldsymbol{\omega}_2(t_2) = c_2 \boldsymbol{\omega}_2(t_1). \quad (19)$$

We then conclude that the constraints at t_1 and t_2,

$$0 = \|\boldsymbol{\omega}_1(t_j) \times \boldsymbol{j}_1\|_2 - \|\boldsymbol{\omega}_2(t_j) \times \boldsymbol{j}_2\|_2, \; \forall \, j \in \{1, 2\}, \quad (20)$$

can only be fulfilled by coordinates $\boldsymbol{j}_1, \boldsymbol{j}_2$ that fulfill

$$0 = |c_1| \, \|\boldsymbol{\omega}_1(t_1) \times \boldsymbol{j}_1\|_2 - |c_2| \, \|\boldsymbol{\omega}_2(t_1) \times \boldsymbol{j}_2\|_2, \quad (21)$$

$$0 = \left(1 - \left|\tfrac{c_1}{c_2}\right|\right) \|\boldsymbol{\omega}_1(t_1) \times \boldsymbol{j}_1\|_2. \quad (22)$$

For the singular case in which $\frac{\|\boldsymbol{\omega}_1(t_1)\|_2}{\|\boldsymbol{\omega}_2(t_1)\|_2} = \frac{\|\boldsymbol{\omega}_1(t_2)\|_2}{\|\boldsymbol{\omega}_2(t_2)\|_2}$, there exist infinitely many solutions to (22). Otherwise, we obtain
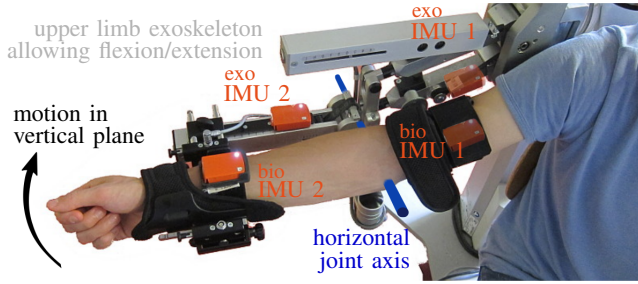
4328

Fig. 2: Validation of joint axis identification in a perfect hinge joint of an exoskeleton and an approximate hinge joint of a human elbow. During the vertical-plane motion both segments rotate simultaneously around the horizontal axis. (Transparency indicates IMUs hidden behind the bar/cuff.)
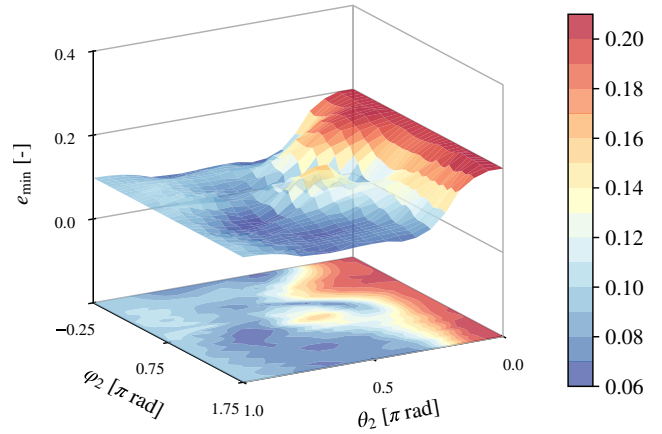

Fig. 3: Reduced error function over spherical coordinates of j_2 for a *motion with fixed joint* of the biological joint. The joint axis coordinates cannot be determined.

two unit-length solutions for j_1, and the signs of j_1, j_2 can be matched just as for the *sequential* motion.

Result 4 (Simultaneous Planar Motions): The joint axis can be determined *up to sign pairing* from data of a *simultaneous planar motion* unless the ratio $\frac{\|\omega_1(t)\|_2}{\|\omega_2(t)\|_2}$ remains constant. If, moreover, the motion contains at least one time instant at which the joint axis is not perfectly horizontal, then the joint axis coordinates can be determined *uniquely* in the sense of Definition 1.

V. EXPERIMENTAL VALIDATION

The theoretical results from Section IV are validated in experimental trials, cf. Figure 2, with two different joints:

- a *mechanical joint*: the perfect hinge joint of an upper limb exoskeleton (Armeo Spring, Hocoma AG) with one IMU attached to each end of the joint, and
- a *biological joint*: the approximate hinge joint of the human elbow with one IMU attached to the distal posterior portion of the upper arm and one IMU attached to the distal portion of the forearm close to the wrist.

The following motions are performed by the biological joint and the mechanical joint simultaneously:

- a *motion with fixed joint*: both segments are moved in three-dimensional space but the relative orientation of the segments remains constant, i.e. the rotational degree of freedom of the joint is not excited,
- a *simultaneous motion in a vertical plane*: the joint axis remains horizontal while both segments rotate simultaneously, and
- a *sequential motion in a horizontal plane*: the joint axis remains vertical while both segments rotate sequentially, i.e. one of them remains fixed while the other rotates, and then vice versa.

All motions are performed smoothly and at comfortable speed, with angular rates below $2\,\frac{\text{rad}}{\text{s}}$ and linear accelerations below $2\,\frac{\text{m}}{\text{s}^2}$, which implies that accelerometer measurements are at least to some extent dominated by gravity. During each motion, the measured accelerations $a_1(t), a_2(t)$ and angular rates $\omega_1(t), \omega_2(t)$ are recorded at $100\,\text{Hz}$. Each motion is conducted for about $40\,\text{s}$ with an additional initial and final rest phase of approximately $10\,\text{s}$, which are used to estimate and remove the gyroscope bias.

As illustrated in Figure 2, the IMUs are carefully attached such that one of the local measurement axes approximately coincides with the functional joint axis during each of the motions. We can therefore determine an approximate ground truth for the coordinates j_1 and j_2, with $\hat{j}_1 \approx [0, 1, 0]^\mathsf{T}, \hat{j}_2 \approx [0, 1, 0]^\mathsf{T}$ for the motion in a vertical plane (cf. Figure 2), and $\hat{j}_1 \approx [0, 1, 0]^\mathsf{T}, \hat{j}_2 \approx [0, 0, 1]^\mathsf{T}$ for the motion in the horizontal plane. While this precise attachment might be easy to realize for the exoskeleton, which exhibits even and orthogonal surfaces and edges, it can only be approximately achieved for the human upper limb. Note furthermore that the human elbow is not perfectly constrained to one rotational degree of freedom and that the IMUs are not rigidly connected to the bones, i.e. soft-tissue motion artifacts may occur.

For both joints and for each of the described motions we investigate whether the proposed kinematic constraints yield a unique pair of axis coordinates j_1 and j_2 near the approximate ground truth. Every tenth sample of the data of a motion is selected, i.e. $t_{k+1} = t_k + 0.1\,\text{s}$. Then, we search for joint axis coordinates that fulfill (8), (9) for each selected sample $t_k, k = 1, ..., N$.

To focus the analysis on (9), we assure (8) by expressing j_1, j_2 in spherical coordinates $(\theta_1, \varphi_1), (\theta_2, \varphi_2)$:

$$j_i = r \begin{bmatrix} \cos(\theta_i) \\ \sin(\theta_i)\sin(\varphi_i) \\ \sin(\theta_i)\cos(\varphi_i) \end{bmatrix}, \ i = 1, 2, \qquad (23)$$

$$\begin{aligned} \theta_1 \in [0, \pi), && \varphi_1 \in [0, \pi), \\ \theta_2 \in [0, \pi), && \varphi_2 \in [0, 2\pi), \end{aligned} \qquad (24)$$

where $r = 1$ to assure the norm constraint (8). Note that j_1 is limited to a hemisphere whereas j_2 covers a full sphere. This assures that the N kinematic constraint equations have a single unique solution in the defined ranges if and only if the joint axis is uniquely identifiable in the sense of Definition 1.
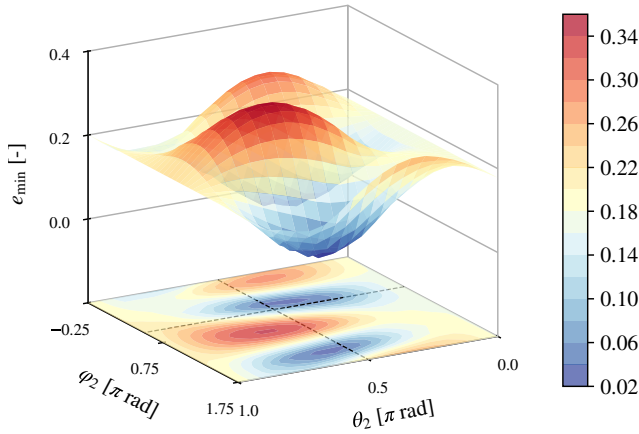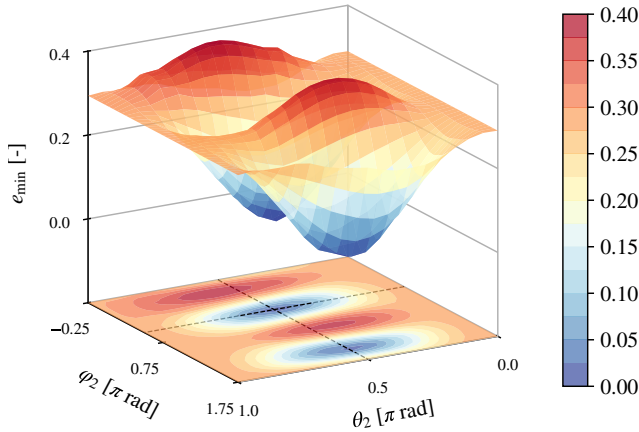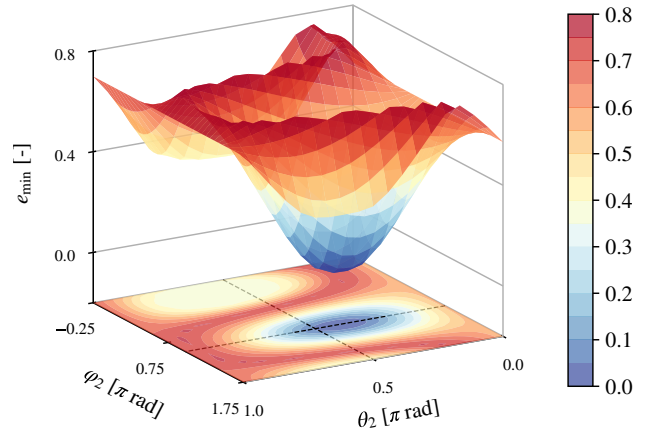
(a) motion performed by biological joint
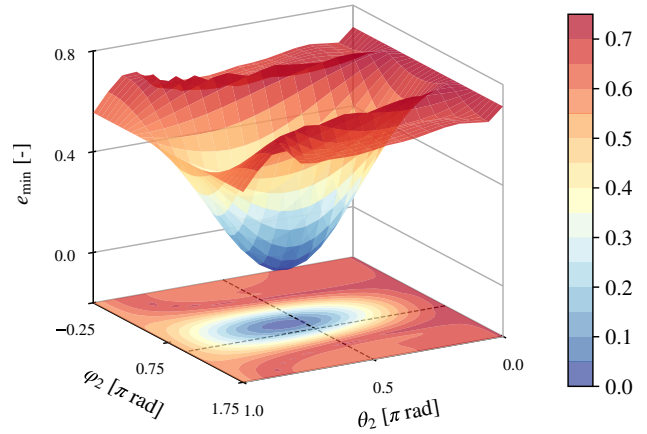
(b) motion performed by mechanical joint

Fig. 4: Reduced error function over spherical coordinates of $\boldsymbol{j}_2$ for a *simultaneous motion in a vertical plane*. The true joint axis (dashed) can be determined up to sign pairing.

(a) motion performed by biological joint

(b) motion performed by mechanical joint

Fig. 5: Reduced error function over spherical coordinates of $\boldsymbol{j}_2$ for a *sequential motion in a horizontal plane*. The true joint axis (dashed) can be determined uniquely.

We define the normalized error function $e(\boldsymbol{j}_1, \boldsymbol{j}_2)$ with

$$e(\boldsymbol{j}_1, \boldsymbol{j}_2) := \frac{\tilde{e}(\boldsymbol{j}_1, \boldsymbol{j}_2)}{\max\limits_{(\boldsymbol{j}_1, \boldsymbol{j}_2)} \tilde{e}(\boldsymbol{j}_1, \boldsymbol{j}_2)}, \tag{25}$$

$$\tilde{e}(\boldsymbol{j}_1, \boldsymbol{j}_2) := \sum_{k=1}^{N} \left(\frac{|h_1(t_k, \boldsymbol{j}_1, \boldsymbol{j}_2)|}{|h_{1,\max}(\boldsymbol{j}_1, \boldsymbol{j}_2)|} + \frac{|h_2(t_k, \boldsymbol{j}_1, \boldsymbol{j}_2)|}{|h_{2,\max}(\boldsymbol{j}_1, \boldsymbol{j}_2)|} \right)$$

$$h_{i,\max}(\boldsymbol{j}_1, \boldsymbol{j}_2) := \max_{k=1}^{N} h_i(t_k, \boldsymbol{j}_1, \boldsymbol{j}_2), i = 1, 2,$$

which is zero if and only if $\boldsymbol{j}_1, \boldsymbol{j}_2$ fulfill (8), (9) for each selected sample $t_k, k = 1, ..., N$. In the presence of small inaccuracies, disturbances and noise, the function $e(\boldsymbol{j}_1(\theta_1, \varphi_1), \boldsymbol{j}_2(\theta_2, \varphi_2))$ should have a global minimum near the approximate ground truth coordinates if the proposed identifiability conditions hold.

The spherical coordinate space is discretized in $10°$-steps, and the error $e(\boldsymbol{j}_1(\theta_1, \varphi_1), \boldsymbol{j}_2(\theta_2, \varphi_2))$ is determined for each point in this four-dimensional grid. To illustrate the shape of

this function, we define the *reduced* error function

$$e_{\min}(\theta_2, \varphi_2) := \min_{\theta_1, \varphi_1} e(\boldsymbol{j}_1(\theta_1, \varphi_1), \boldsymbol{j}_2(\theta_2, \varphi_2)), \tag{26}$$

which should exhibit a global minimum near the approximate ground truth coordinates if the proposed identifiability conditions hold.

Figures 3, 4 and 5 illustrate $e_{\min}(\theta_2, \varphi_2)$ for the three performed motions of the biological and the mechanical joint. The approximated ground truth coordinates are indicated by horizontal lines in Figures 4 and 5. To avoid global minima lying exactly on the edge of the plotted surface, we plot φ_2 over $[-\frac{1}{4}\pi, \frac{7}{4}\pi)$ instead of $[0, 2\pi)$.

Figure 3 shows results for the *motion with fixed joint*. As expected, the reduced error remains small over all θ_2, φ_2 and varies only slightly due to measurement noise and inaccuracies of the joints or the motion. This agrees well with the theoretical Result 1 that the kinematic constraints do not yield a unique joint axis for the considered motion.

Figure 4 presents results for the *simultaneous motion in*

4330

a vertical plane. For both the mechanical and the biological joint, there are two distinct minima with very similar error function values. One occurs near the true coordinates $(\hat{\boldsymbol{j}}_1, \hat{\boldsymbol{j}}_2)$, the other is shifted by π in the φ_2-dimension, i.e. it occurs near the axis coordinates $(\hat{\boldsymbol{j}}_1, -\hat{\boldsymbol{j}}_2)$, which are only correct up to non-matching signs. This is in accordance with the theoretical Result 4 for the motion in a vertical plane. Note that the minimum values for the mechanical joint are almost zero, while the minima have slightly larger values for the biological joint and occur at coordinates that are slightly different from the approximate ground truth. This could be due to imperfect sensor-to-segment alignment, imperfect joint kinematics, and soft tissue motion.

Figure 5 shows results for a *sequential motion in a horizontal plane*. The error function of the mechanical joint exhibits a global minimum near the approximate ground truth. In the light of Results 3 and 4, the direct comparison of Figures 5b and 4b shows that the accelerometer-based constraint helps to match the signs of $\boldsymbol{j}_1$ and $\boldsymbol{j}_2$ only if the joint axis is not horizontal. For the biological joint, this result is confirmed. However, as for the vertical-plane motion, the minimum error function value is slightly larger, and the approximate ground truth is less accurate.

For the sake of completeness, we also evaluated the error

$$e_{\min}(\theta_1, \varphi_1) := \min_{\theta_2, \varphi_2} e(\boldsymbol{j}_1(\theta_1, \varphi_1), \boldsymbol{j}_2(\theta_2, \varphi_2)) \qquad (27)$$

and found equally shaped global minima, which is not surprising, since all constraints are symmetric in $\boldsymbol{j}_1$ and $\boldsymbol{j}_2$.

VI. CONCLUSIONS

In this work, we have considered joint axis identification in (approximate) hinge joints. We have introduced a novel acceleration-based kinematic constraint and combined it with an existing gyroscope-based constraint. Furthermore, we have derived a simple rank condition under which the joint axis coordinates are uniquely identifiable. For two common motion patterns, i.e. sequential and planar motions, we have shown that identifiability is assured, with the minor exception that the signs cannot be matched if the joint axis remains perfectly horizontal during the entire motion. We have validated these theoretical results in experiments using both a biological and a mechanical joint.

Future research will focus on a more detailed analysis of the contributions of the accelerometer- and the gyroscope-based constraints and on strategies for optimal combination of both [20]. Furthermore, we will analyze the accuracy of the estimated joint axis coordinates and kinematic parameters calculated from them. Finally, we would like to extend the scope to kinematic constraints for two-dimensional joints and to kinematic chains with more degrees of freedom [2], [18].

REFERENCES

[1] A. Filippeschi, N. Schmitz, M. Miezal, G. Bleser, E. Ruffaldi, and D. Stricker, "Survey of motion tracking methods based on inertial sensors: A focus on upper limb human motion," *Sensors*, vol. 17, no. 6, 2017.

[2] M. Kok, J. D. Hol, and T. B. Schön, "An optimization-based approach to human body motion capture using inertial sensors," in *IFAC Proceedings Volumes*, vol. 47, no. 3, 2014, pp. 79 – 85, 19th IFAC World Congress.

[3] V. R. Marco, J. Kalkkuhl, and T. Seel, "Nonlinear observer with observability-based parameter adaptation for vehicle motion estimation," in *Proceedings of the 18th IFAC Symposium on System Identification, (SYSID)*, Stockholm, Sweden, 2018, pp. 60–65.

[4] G. Dissanayake, S. Sukkarieh, E. Nebot, and H. Durrant-Whyte, "The aiding of a low-cost strapdown inertial measurement unit using vehicle model constraints for land vehicle applications," *IEEE transactions on robotics and automation*, vol. 17, no. 5, pp. 731–747, 2001.

[5] N. Roy, P. Newman, and S. Srinivasa, *State Estimation for Legged Robots: Consistent Fusion of Leg Kinematics and IMU.* MITP, 2013.

[6] S. Leutenegger, S. Lynen, M. Bosse, R. Siegwart, and P. Furgale, "Keyframe-based visual–inertial odometry using nonlinear optimization," *The International Journal of Robotics Research*, vol. 34, no. 3, pp. 314–334, 2015.

[7] M. Hassan, H. Kadone, K. Suzuki, and Y. Sankai, "Wearable gait measurement system with an instrumented cane for exoskeleton control," *Sensors*, vol. 14, no. 1, pp. 1705–1722, 2014.

[8] T. Seel, D. Laidig, M. Valtin, C. Werner, J. Raisch, and T. Schauer, "Feedback control of foot eversion in the adaptive peroneal stimulator," in *Proceedings of the 22nd IEEE Mediterranean Conference on Control and Automation*, Palermo, Italy, 2014, pp. 1482–1487.

[9] J. Favre, B. Jolles, R. Aissaoui, and K. Aminian, "Ambulatory measurement of 3D knee joint angle," *Journal of biomechanics*, vol. 41, pp. 1029–1035, 02 2008.

[10] J. Favre, R. Aissaoui, B. Jolles, J. de Guise, and K. Aminian, "Functional calibration procedure for 3D knee joint angle description using inertial sensors," *Journal of Biomechanics*, vol. 42, no. 14, pp. 2330–2335, 2009.

[11] A. Cutti, A. Ferrari, P. Garofalo, M. Raggi, A. Cappello, and A. Ferrari, "'Outwalk': A protocol for clinical gait analysis based on inertial and magnetic sensors," *Medical & biological engineering & computing*, vol. 48, pp. 17–25, 11 2009.

[12] T. Seel, J. Raisch, and T. Schauer, "IMU-based joint angle measurement for gait analysis," *Sensors*, vol. 14, no. 4, pp. 6891–6909, 2014.

[13] B. Taetz, G. Bleser, and M. Miezal, "Towards self-calibrating inertial body motion capture," in *Proceedings of the 19th International Conference on Information Fusion*, Heidelberg, Germany, Jul. 2016, pp. 1751–1759.

[14] T. Seel, T. Schauer, and J. Raisch, "Joint axis and position estimation from inertial measurement data by exploiting kinematic constraints," in *Proceedings of the IEEE Multi-Conference on Systems and Control*, Dubrovnik, Croatia, 2012, pp. 45–49.

[15] D. Laidig, T. Schauer, and T. Seel, "Exploiting kinematic constraints to compensate magnetic disturbances when calculating joint angles of approximate hinge joints from orientation estimates of inertial sensors," in *Proc. of 15th IEEE Conference on Rehabilitation Robotics (ICORR)*, London, UK, 2017, pp. 971–976.

[16] F. Olsson and K. Halvorsen, "Experimental evaluation of joint position estimation using inertial sensors," in *2017 20th International Conference on Information Fusion (Fusion)*, July 2017, pp. 1–8.

[17] P. Müller, M. A. Bégin, T. Schauer, and T. Seel, "Alignment-free, self-calibrating elbow angles measurement using inertial sensors," *IEEE Journal of Biomedical and Health Informatics*, vol. 21, no. 2, pp. 312–319, 2017.

[18] D. Laidig, P. Müller, and T. Seel, "Automatic anatomical calibration for IMU-based elbow angle measurement in disturbed magnetic fields," *Current Directions in Biomedical Engineering*, vol. 3(2), pp. 167–170, 2017.

[19] A. Küderle, S. Becker, and C. Disselhorst-Klug, "Increasing the robustness of the automatic imu calibration for lower extremity motion analysis," *Current Directions in Biomedical Engineering*, vol. 4, pp. 439–442, 2018.

[20] F. Olsson, T. Seel, D. Lehmann, and K. Halvorsen, "Joint axis estimation for fast and slow movements using weighted gyroscope and acceleration constraints," in *International Conference on Information Fusion*, 2019. [Online]. Available: https://arxiv.org/abs/1903.07353